



RESEARCH ARTICLE - ENGINEERING (MISCELLANEOUS)

Diagnostic of Osteoporosis Using Backpropagation Neural Networks

Falah A. Bida¹, Hayder A. Naser^{2*}

¹Directorate of Education in Baghdad / Rusafa III, Ministry of Education, Baghdad, Iraq

²Department of Computer Techniques Engineering, Imam Al-Kadhum University College, Baghdad, Iraq

* Corresponding author E-mail: hayder.a.naser@gmail.com

Article Info.	Abstract
<p><i>Article history:</i></p> <p>Received 24 June 2024</p> <p>Accepted 17 October 2024</p> <p>Publishing 30 June 2025</p>	<p>In this study, an artificial neural network (ANN) using backpropagation was utilized to categorize bone images into either healthy or osteoporotic categories based on various statistical operations. An input matrix was constructed containing the six statistical features of 125 samples, representing X-ray images of knee joints, with 25 healthy and 100 osteoporotic samples. Of these, 70% were used for training, 15% for validation, and 15% for network testing. The classification efficiency of the neural network for the 125 samples was 97%. The research included analysis of arithmetic mean, standard deviation, variance, energy, homogeneity, and entropy values for the healthy bone samples. The backpropagation neural network (BNN) was trained with six inputs (representing the six statistical features), 80 hidden layers, and five outputs (two for healthy and three for osteoporotic conditions). A comparison of K-Nearest Neighbors (KNN), Logistic Regression, and BNN techniques applied to 2,350 images revealed that BNNs achieved the highest accuracy. This network has the potential to assist healthcare providers in both detecting the early stages of osteoporosis and developing appropriate treatment plans.</p>
<p>This is an open-access article under the CC BY 4.0 license (http://creativecommons.org/licenses/by/4.0/)</p>	
<p>Publisher: Middle Technical University</p>	
<p>Keywords: Backpropagation Neural Networks (BNN); Osteoporosis; Digital Image Processing; Statistical Operations; Artificial Neural Network (ANN).</p>	

1. Introduction

The subject of digital image processing techniques plays an important role in all types of medicine, whether in diagnosis or treatment. With the rapid development in the medical field, what is known as the “electronic doctor” has become a reality that can be trusted to a high degree and is an important factor in detecting and diagnosing many diseases accurately. Detecting diseases early can facilitate quicker recovery and potentially prevent many conditions, particularly cancers. The role of these systems is growing with the great progress in medical imaging methods using computers, which produce huge amounts of data that need someone to interpret them and extract information from them to diagnose diseases quickly and effectively [1]. Human bone consists of a solid outer part, a network of fibers called trabecular bone, and the inner part in most bones is hollow and requires sufficient space for marrow cavities. Bones are initially composed of cartilage, then the body deposits calcium in the cartilage to form bones, and some cartilage will eventually remain for peace and tolerance between the bones, and thus cartilage with some pillars and other tissues strengthens the articulation between bones, and cartilage is blessed with the presence of a cushion at the end of some bones as part of the diversity [2]. Osteoporosis is a progressive, systemic, and skeletal disease that is characterized by low bone mass and microarchitectural deterioration of bone tissue, leading to increased bone fragility and consequent increase in fracture risk [3]. The peak bone mass in young adulthood depends largely on genetic, biological, and lifestyle factors since low bone strength during the growing years is associated with increased fragility fracture risk during old age [4]. It is reported that bone loss starts from the age of 30–40 years in both men and women [5]. In women, a marked increase in bone loss during premenopausal and postmenopausal periods is observed, while in men, a small longitudinal bone loss is observed throughout life [6, 7]. Numerous techniques have been used to study osteoporosis in the past, including artificial neural network (ANN) [8], Dual-Energy X-ray absorptiometry DEXA [9], deep convolutional neural networks [10], Squirrel Search Algorithm (SSA) based Deep Convolutional Neural Networks (DCNNs) [11], nGLCM techniques [12] and convolutional neural networks (CNNs) [13]. Additionally, BNNs have shown potential in pre-validating existing and new financial imbalances [14], suggesting broader applications for this type of model. Given that the issue of osteoporosis is one of the important topics in bone pathology, in addition to its widespread spread in different countries, the need arose for a quick and inexpensive method to help people detect this disease. Therefore, we proposed in the current research the application of statistical analysis methods for digital images using ANN and the MATLAB 2020 program to predict osteoporosis from healthy images representing bone samples found in X-ray laboratories.

The structure of this research is organized as follows: Section 2 is dedicated to describing the methodology of the study, followed by the statistical and BNN training results. Finally, a demonstration of the process is provided, compared with other algorithms, and conclusions are listed.

Nomenclature & Symbols			
DEXA	Dual-Energy X-Ray Absorptiometry	CNNs	Convolutional Neural Networks
ANN	Artificial Neural Network	BNN	Backpropagation Neural Network
SSA	Squirrel Search Algorithm	GUI	Graphical User Interface
DCNNs	Deep Convolutional Neural Networks	KNN	K-Nearest Neighbors
AUC	Area Under the Curve	CA	Classification Accuracy
MCC	Matthews Correlation Coefficient	X	Arithmetic Mean
VAR	Variance	H	Homogeneity
std	Standard Deviation	E	Entropy

2. Methodology

2.1. Samples and image

The methodology presented in this study represents the calculation of statistical processes for 100 normal images and 25 osteoporosis images to train the neural network to distinguish between healthy and diseased images. Fig. 1 (a, b) shows a group of images of healthy and osteoporotic bones.

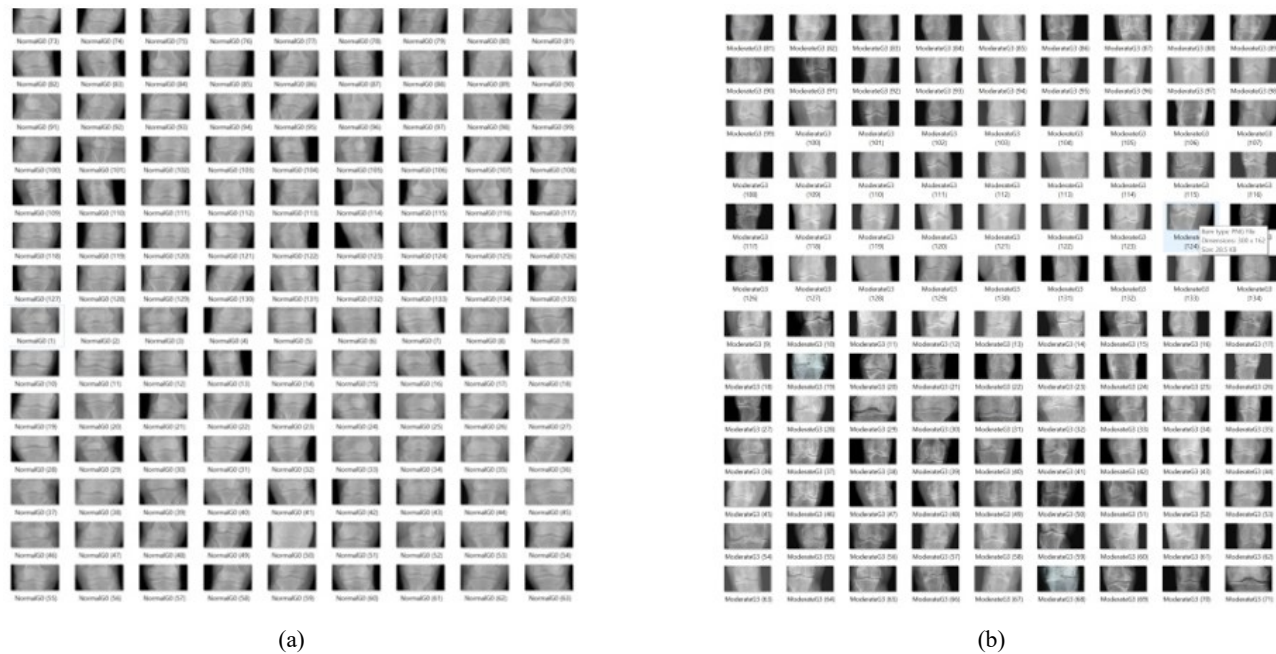


Fig. 1. (a) normal image, (b) osteoporosis image

2.2. Artificial Neural Networks (ANN)

The key to the artificial neural network (ANN) model is the structure of the information processor system that connects and organizes a large number of internally connected processing elements (neurons) that work in harmony to solve specific problems. Signals pass between nodes (neurons) via connection lines, and each line is accompanied by a weight. The signals entering the node (neuron) are multiplied by these weights, and the weighted inputs are collected in the nodes or neurons, and then the outputs of each node are processed by a non-linear function with a certain threshold (Threshold) known as the activation function [15].

2.3. Backpropagation Neural Network (BNN)

It has become the mainstay of neural computers (neurocomputing) and has successful applications in wide areas for solving dilemmas, including applications for signal filtering, pattern recognition, and image focusing. This type of neural network has a solid mathematical basis, and neural networks with backpropagation can tackle any problem related to the field of patterns, as the network processes the in-pattern and extracts a coherent out-pattern [16]. Fig. 2 represents the process of forward passage of the activation node through the ANN from the input nodes, and backward propagation from the output nodes to the input nodes [17].

2.4. Pattern recognition using ANN

Pattern recognition or recognizing models is one of the branches of artificial intelligence. Pattern recognition can be defined as classifying input data that determines their identity by extracting the important properties, features, or bodies of the data, meaning that it is any program that treats the image and gives a classification or identification of the images, as shown in Fig. 3 [18, 19].

2.5. Statistical operations

In studying the bones under investigation, will need some important statistical measures, where the statistical characteristics of each image of the study samples are calculated, through which the neural network will be able to distinguish between the infected and healthy samples, which are as follows [20]:

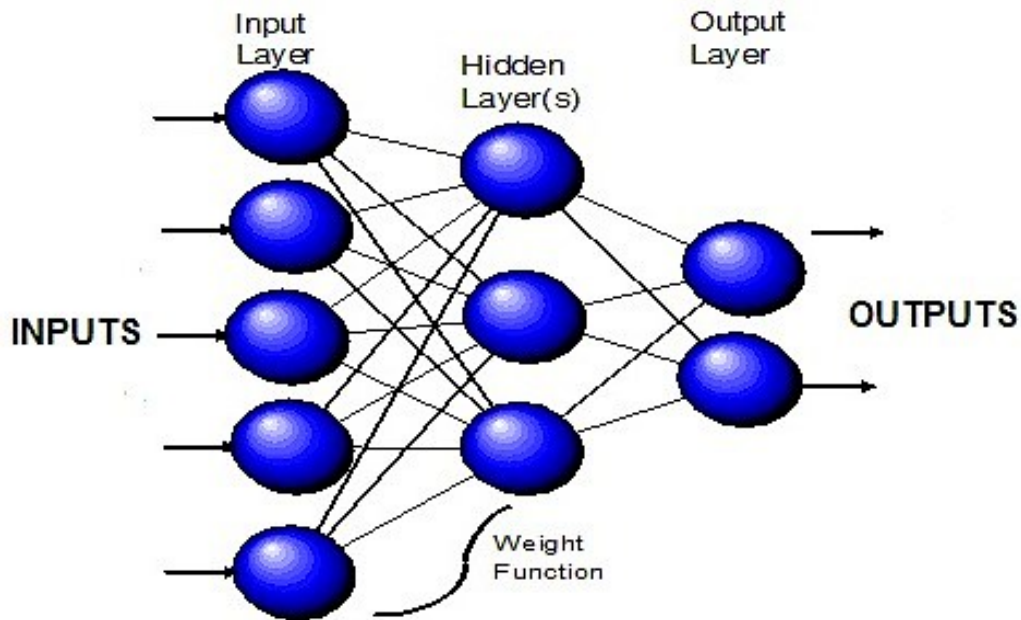


Fig. 2. Backpropagation neural network (BNN) [17]

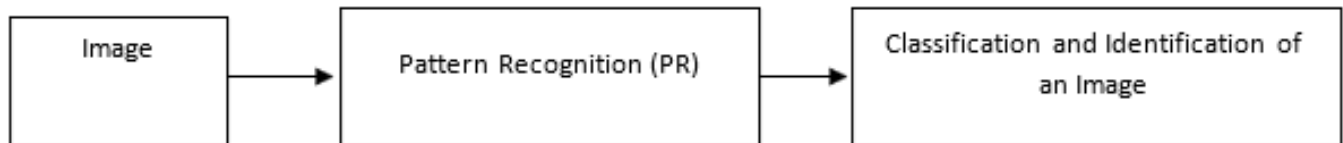


Fig. 3. Shows the pattern recognition system [19]

2.5.1. Arithmetic mean

The arithmetic mean is the sum of the intensity values of the image elements divided by their number (n), and the equation represents it:

$$\bar{X} = \frac{\sum_{i=1}^n X_i}{n} \tag{1}$$

2.5.2. Variance

Variance is the average sum of the squares of the deviations of the values, and it is represented by the equation:

$$VAR = \frac{\sum(X-\bar{X})^2}{n-1} \tag{2}$$

2.5.3. Standard deviation

Standard deviation is the positive square root of the variance, and it is represented by the equation:

$$\text{std} = \sqrt{VAR} = \sqrt{\frac{\sum(x_i-\bar{x})^2}{n-1}} \tag{3}$$

2.5.4. Energy

Energy measures how the light intensity is distributed in the image, and it is represented by the equation:

$$\text{Energy} = \sum_{i,j} f(i,j)^2 \tag{4}$$

2.5.5. Homogeneity

Homogeneity refers to the distribution of elements in the grayscale image, and the equation represents it:

$$H = \sum_{i,j} \frac{f(i,j)}{1+|i-j|} \tag{5}$$

2.5.6. Entropy(E)

Entropy (E) is a statistical measure that expresses the irregularity in the components of the image. It is used as a standard of quality and can be calculated by:

$$E = -\sum (f(i,j) \log_2 f(i,j)) \tag{6}$$

3. Practical Aspect

ANN algorithm with the inverse relationship:

- Creating a strategic innovation network by identifying six input levels, 80 hidden levels, and five output levels.
- Giving indirect value to inputs and weights.
- Use the inverse exercise method to adjust the weights, and temporary values, and calculate the error value.
- Repeat step 3 until an acceptable error value is reached.
- Use some surprising results to train the network on them.
- Examine the network to ensure that it distributes the specified categories. Fig. 4 represents the synthetic network used.

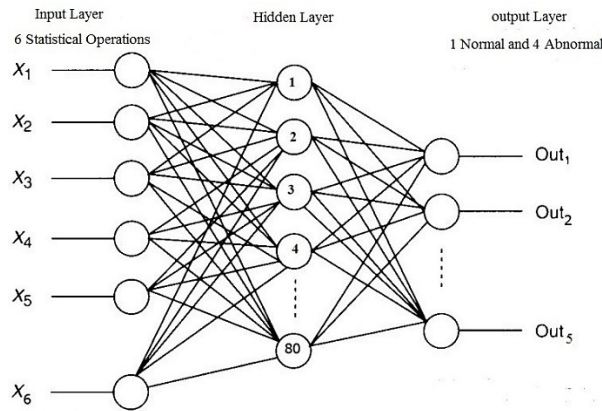


Fig. 4. Represents the ANN used in this work

Figs. 5 and 6 show the flow chart for training ANN. Figs. 7 and 8 show the graphical user interface (GUI) for the preliminary processing and statistical operations of one of the study samples.

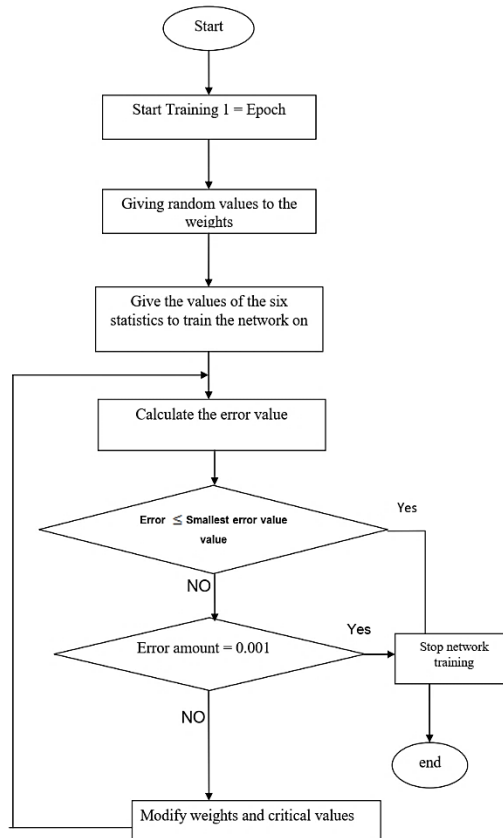


Fig. 5. Shows the flow chart for training a back-propagation artificial neural network

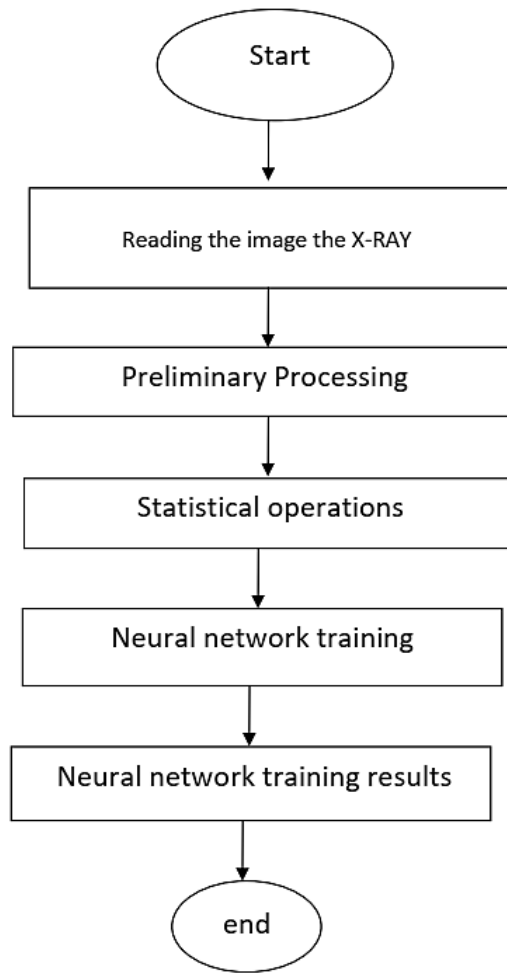


Fig. 6. The flowchart of the study model

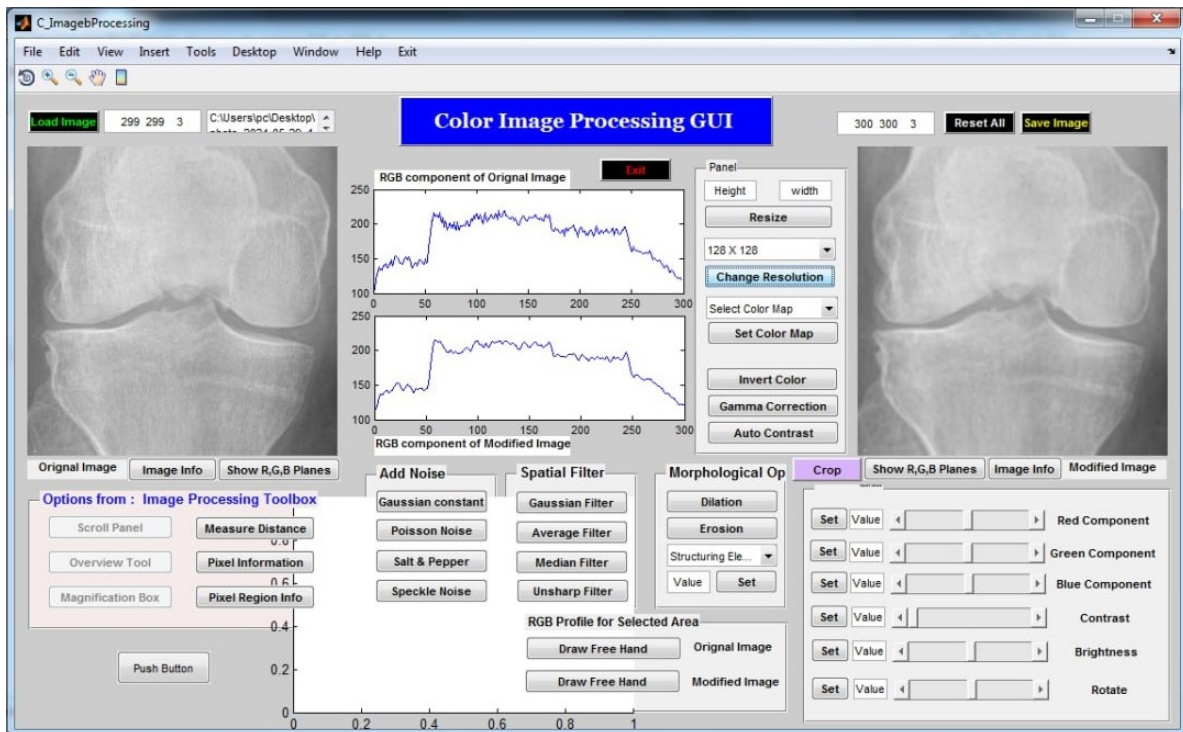


Fig. 7. Graphical user interface (GUI) for the preliminary processing of one of the study samples

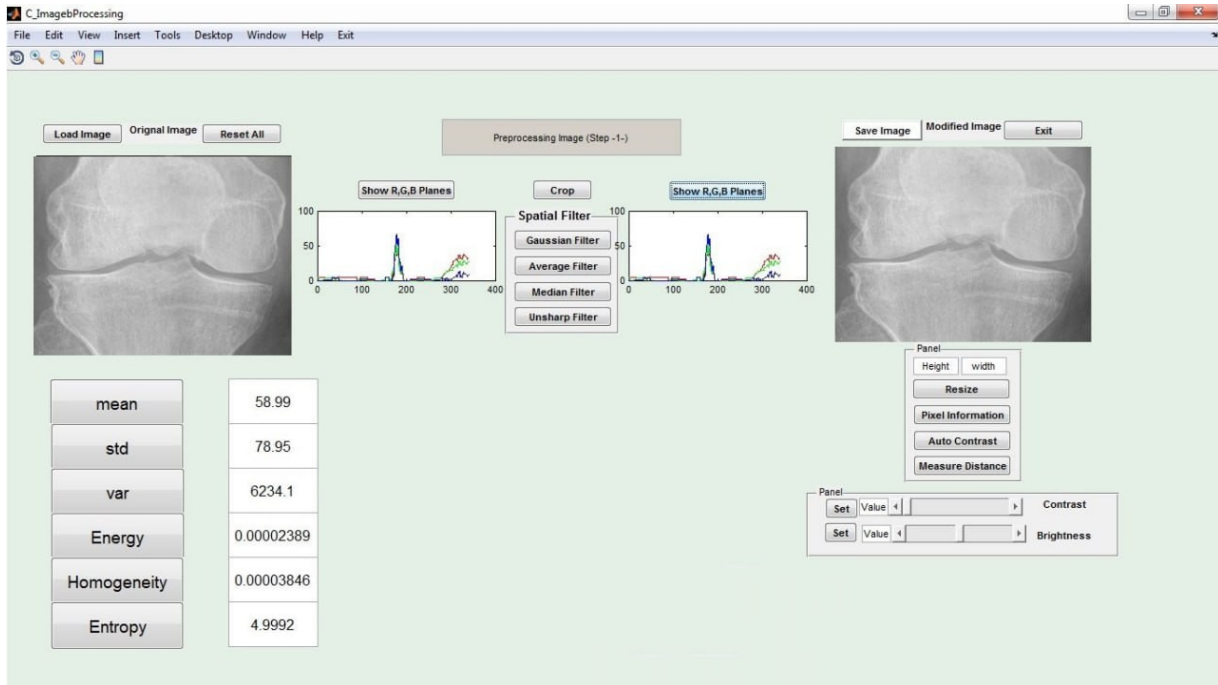


Fig. 8. Graphical user interface (GUI) for the statistical operations

3.1. Statistical results

Tables 1 and 2 show the results of applying statistical operations in equations (1 to 6) on the study images, which number 25 images representing healthy bone samples and 100 images representing osteoporosis bone samples. In these tables, a set of special features is extracted through statistical operations such as arithmetic mean, standard deviation, variance, power, homogeneity, and entropy to classify research samples into infected and healthy by training the neural network.

Table 1. Values of the arithmetic mean, standard deviation, variance, energy, homogeneity, and entropy for the study/normal samples

Samples No.	normal samples					
	Mean	Std	VAR	Energy	Homogeneity	Entropy
.1	226.38	168.01	27898.3	0.000009929	0.00007319	7.9138
.2	227.66	156.74	24258.9	0.000009866	0.00007473	9.5275
.3	228.64	137.11	18258.7	0.000009801	0.00007609	9.7594
.4	234.26	178.47	31496.6	0.000009877	0.00007447	9.1256
.5	231.55	163.33	26358.0	0.000008887	0.00007705	9.4079
.6	235.12	155.45	23857.8	0.000008821	0.00007975	9.5873
.7	234.98	156.68	24239.2	0.000009302	0.00008552	9.7375
.8	238.05	157.57	24519.1	0.000009335	0.00008672	9.9844
.9	239.98	159.55	25188.1	0.000009571	0.00009418	9.8336
.10	237.48	155.65	23919.6	0.000009183	0.00009899	9.8164
.11	239.07	158.25	24728.5	0.000009351	0.00009826	9.9304
.12	239.92	162.44	26069.8	0.000009401	0.00009848	9.8278
.13	242.35	164.23	26647.0	0.000009679	0.00008062	9.2748
.14	241.37	166.35	27341.6	0.000009422	0.00008377	9.4221
.15	248.43	169.96	28683.8	0.000009207	0.00008407	9.5657
.16	246.97	175.51	30454.7	0.000009418	0.00008498	9.7303
.17	249.44	176.69	30867.9	0.000009433	0.00008566	9.9594
.18	249.96	177.86	31279.9	0.000009573	0.00008799	9.8475
.19	252.57	171.07	28924.8	0.000008302	0.00008816	9.8526
.20	251.74	169.98	28856.8	0.000008455	0.00009369	9.8201
.21	254.22	165.94	27206.2	0.000008528	0.00009506	9.8337
.22	251.78	163.26	26329.3	0.000008783	0.00009661	9.8428
.23	259.90	156.63	24224.6	0.000008871	0.00009808	9.8033
.24	255.55	151.12	22537.0	0.000008973	0.00009931	9.8499
.25	261.52	151.06	22519.0	0.000008978	0.00009944	9.8395

Table 2. Shows the values of the arithmetic mean, standard deviation, variance, energy, homogeneity, and entropy for the study samples afflicted with osteoporosis

No. Osteoporosis	Mean	Std	VAR	Energy	Homogeneity	Entropy
1	226.38	168.01	27893.3	0.00009829	0.00007319	9.9138
2	227.66	156.74	24255.9	0.00009866	0.00007473	9.5275
3	229.94	136.11	18255.7	0.00009701	0.00007609	9.7594
4	234.26	178.47	31496.6	0.00009877	0.00007447	9.1256
5	231.55	163.33	26352.0	0.00009387	0.00007705	9.4079
6	235.12	155.45	23855.8	0.00009621	0.00007975	9.5873
7	235.86	156.68	24237.2	0.00009302	0.00008552	9.7375
8	238.05	157.57	24514.1	0.00009335	0.00008672	9.9844
9	239.98	159.55	25139.1	0.00009571	0.00009418	9.9336
10	237.48	155.65	23917.6	0.00009183	0.00009899	9.9164
11	239.07	158.25	24728.5	0.00009351	0.00009826	9.9304
12	239.92	162.44	26063.8	0.00009401	0.00009848	9.9278
13	242.35	164.23	26645.0	0.00009679	0.00008062	9.2748
14	245.37	166.35	27341.6	0.00009422	0.00008377	9.4221
15	248.43	169.86	28683.8	0.00009207	0.00008407	9.5657
16	246.97	175.51	30454.7	0.00009418	0.00008498	9.7303
17	248.44	176.69	30867.9	0.00009433	0.00008566	9.9594
18	249.86	177.86	31279.8	0.00009573	0.00008799	9.3475
19	252.57	171.07	28924.8	0.00008302	0.00008816	9.9526
20	251.74	169.98	28856.8	0.00008455	0.00009369	9.7201
21	254.22	165.94	27206.2	0.00008528	0.00009506	9.9337
22	258.78	163.26	26329.3	0.00008783	0.00009661	9.8428
23	259.90	156.63	24221.6	0.00008871	0.00009808	9.7033
24	255.55	151.12	22537.0	0.00008973	0.00009931	9.8499
25	261.52	151.06	22519.0	0.00008978	0.00009944	9.9395
26	72.21	91.50	8191.2	0.00006294	0.00003390	8.6440
27	75.94	89.97	8005.8	0.00006517	0.00005662	8.5892
28	77.17	59.01	3366.1	0.00006103	0.00006558	8.5175
29	82.78	89.80	7886.4	0.00007224	0.00005397	8.3922
30	79.99	82.66	6669.3	0.00007115	0.00004660	8.2760
31	85.01	91.87	9192.1	0.00007043	0.00003048	8.1415
32	89.09	91.09	8117.2	0.00005564	0.00007140	7.7552
33	86.82	98.08	9425.5	0.00005931	0.00007004	7.5606
34	88.47	98.26	8512.9	0.00006306	0.00006903	7.3441
35	85.57	97.41	9295.8	0.00005810	0.00006893	7.1255
36	91.17	91.47	8185.8	0.00005682	0.00006810	7.4074
37	93.16	88.24	7611.8	0.00005287	0.00006779	7.8485
38	94.65	94.27	8699.8	0.00006331	0.00006223	8.2696
39	96.76	99.75	9752.5	0.00006530	0.00005417	8.3249
40	99.61	99.93	9947.7	0.00006490	0.00003222	8.2890
41	98.24	98.48	9503.3	0.00006401	0.00003684	8.3028
42	91.38	95.39	8919.4	0.00006826	0.00003018	8.3227
43	101.69	89.40	7815.5	0.00007269	0.00003717	8.3672
44	102.14	92.77	8422.7	0.00007500	0.00004376	8.4066
45	106.77	99.17	9638.3	0.00007737	0.00004690	8.4558
46	104.06	96.93	9203.5	0.00007037	0.00004881	8.4622
47	105.17	98.47	9501.4	0.00006809	0.00005077	8.4873
48	112.92	97.38	9290.1	0.00006419	0.00005898	8.5218
49	107.39	92.44	8362.2	0.00006206	0.00006605	8.5306
50	108.06	96.66	9151.8	0.00006166	0.00007060	8.5462
51	70.99	79.95	6235.1	0.00004389	0.00004846	7.9992
52	72.34	65.57	4170.2	0.00007387	0.00003406	7.5735
53	73.57	67.17	4379.4	0.00007852	0.00003577	7.3765
54	74.61	67.75	4457.6	0.00007568	0.00003634	8.3288
55	78.45	84.73	7019.8	0.00007428	0.00003733	8.5039
56	77.57	77.38	5834.9	0.00007251	0.00003904	8.1696
57	76.24	75.25	5515.0	0.00007557	0.00004791	7.9210
58	80.27	78.37	5987.5	0.00007381	0.00004656	7.6114
59	82.44	88.96	7737.9	0.00007687	0.00003881	8.7456
60	89.83	72.97	5181.9	0.00007042	0.00004111	8.5475
61	87.72	72.02	5044.8	0.00006733	0.00004342	7.9646
62	88.36	71.99	5040.5	0.00006615	0.00004517	8.8476
63	89.14	71.77	5009.5	0.00006434	0.00003608	8.2421
64	84.98	69.96	4797.9	0.00007177	0.00003572	8.3357

Continue Table 2. Shows the values of the arithmetic mean, standard deviation, variance, energy, homogeneity, and entropy for the study samples afflicted with osteoporosis

65	90.69	70.98	4898.2	0.000006355	0.00006122	7.2862
66	91.26	72.47	5108.9	0.000007946	0.00006639	8.7351
67	95.27	73.48	5254.3	0.000006224	0.00007303	8.2756
68	96.20	74.44	5394.4	0.000006434	0.00007511	8.2387
69	94.36	75.22	5510	0.000004762	0.00007793	7.9256
70	99.47	74.54	5409.1	0.000007434	0.00007508	8.3672
71	99.98	74.11	5346.0	0.000006774	0.00007431	7.7846
72	101.51	73.75	5293.5	0.000005432	0.00007722	8.6148
73	106.58	72.23	5076.1	0.000005548	0.00007156	7.6080
74	110.93	51.78	2579.6	0.000007173	0.00006528	7.6221
75	108.34	50.69	2470.0	0.000004154	0.00006793	8.7781
76	96.90	54.65	2880.1	0.000009255	0.00002199	8.2530
77	97.93	57.43	3194.6	0.000009588	0.00002665	8.1184
78	98.58	56.66	3099.0	0.000008411	0.00003958	8.0086
79	99.57	63.07	3953.1	0.000009978	0.00005451	7.9573
80	99.98	76.11	5643.5	0.000009291	0.00005071	7.7257
81	106.72	72.31	5086.1	0.000008226	0.00005105	7.6636
82	103.52	71.59	4983.9	0.000007882	0.00005404	7.7334
83	104.83	69.55	4699.9	0.000008058	0.00007551	7.6484
84	102.63	63.68	3929.7	0.000008477	0.00005335	7.2256
85	109.51	61.36	3644.3	0.000009637	0.00005698	8.3368
86	111.18	60.53	3544.8	0.000009414	0.00004931	8.3821
87	118.58	57.16	3154.9	0.000009566	0.00004161	7.2203
88	115.16	56.68	3101.2	0.000009443	0.00004711	7.1099
89	116.92	55.25	2944.0	0.000008755	0.00004966	8.5537
90	112.47	50.38	2439.7	0.000008069	0.00004721	7.5114
91	119.30	71.14	5205.9	0.000008039	0.00002185	8.2955
92	120.55	85.79	7189.9	0.000008624	60.0000215	8.7737
93	121.05	62.01	3723.7	0.000008340	0.00003365	8.6369
94	125.36	64.75	4065.0	0.000008664	0.00003466	7.3062
95	123.47	66.13	4242.9	0.000009225	0.00003631	7.5347
96	121.73	68.58	4568.0	0.000009947	0.00004441	7.8376
97	124.38	70.27	47989.3	0.000009073	0.00005205	8.2055
98	127.26	71.37	4951.9	0.000008833	0.00007011	8.3866
99	128.69	73.68	5282.3	0.000008567	0.00007039	8.4466
100	129.88	76.74	5736.8	0.000008186	0.00007041	8.5000

The results of this study, in which we used X-ray images, were compared with [21] which used CT images, and the study most similar to a group of Statistical Operations appears in Table 3.

Table 3. Comparison of the results with previous studies

Ref.	energy	Homogeneity	entropy
The proposed work	6.1255- 9.6304	0.0000639 - 0.00009648	6.6080 - 9.6440
[21]	0.2344-0.5454	0.6302-0.8889	2.7036-3.9166

3.2. BNN Training results

The BNN was trained to consist of six inputs (representing the six statistical features), (80) hidden layers, and five outputs (representing 2 healthy and 3 affected by osteoporosis). An input matrix was used, containing the six statistical features of (125) samples representing an X-ray image of the knee joint from the study samples, (25) of which were healthy and (100) of which were affected by osteoporosis. (70%) of these samples were taken to train the network, (15%) to verify the validity of the training, and (15%) to test the network, as in Fig. 9.

The process of training the neural network is shown in Fig. 10. The neural network classification efficiency for the 125 samples appeared to be 97%, as in Fig. 11.

Fig. 10 shows four groups indicating the results of training, validation, testing, and the final result (All matrix), where each group (Blocks) consists of 25 squares: 12 red squares representing errors, 4 green squares indicating correct results, 8 black squares indicating the percentage of correct results (in green) and incorrect results (in red) for each case, and one blue box indicating the percentage of correct and incorrect samples. In Fig. 11, we can see the result in the All-confusion matrix: the training accuracy is 97% for classifying each case, with an error rate of 3%.

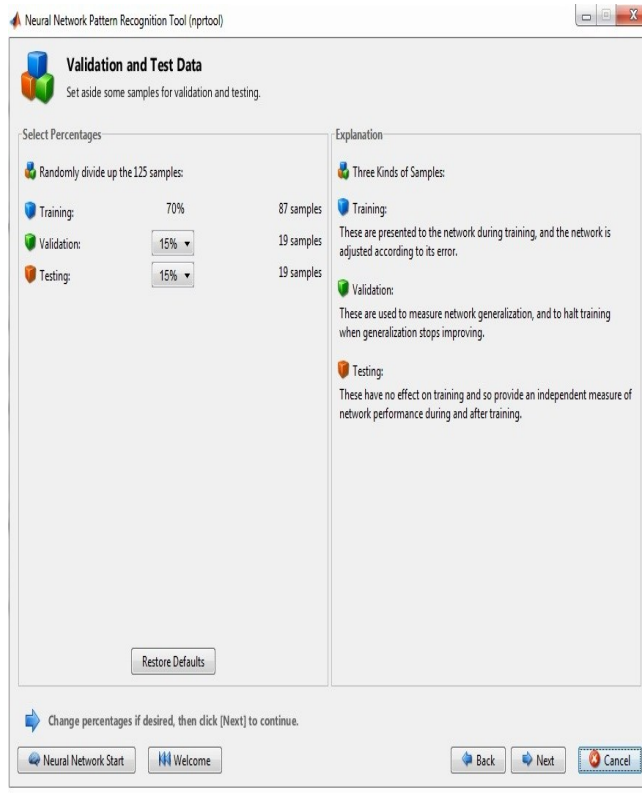


Fig. 9. Choosing training, validation, and testing ratios

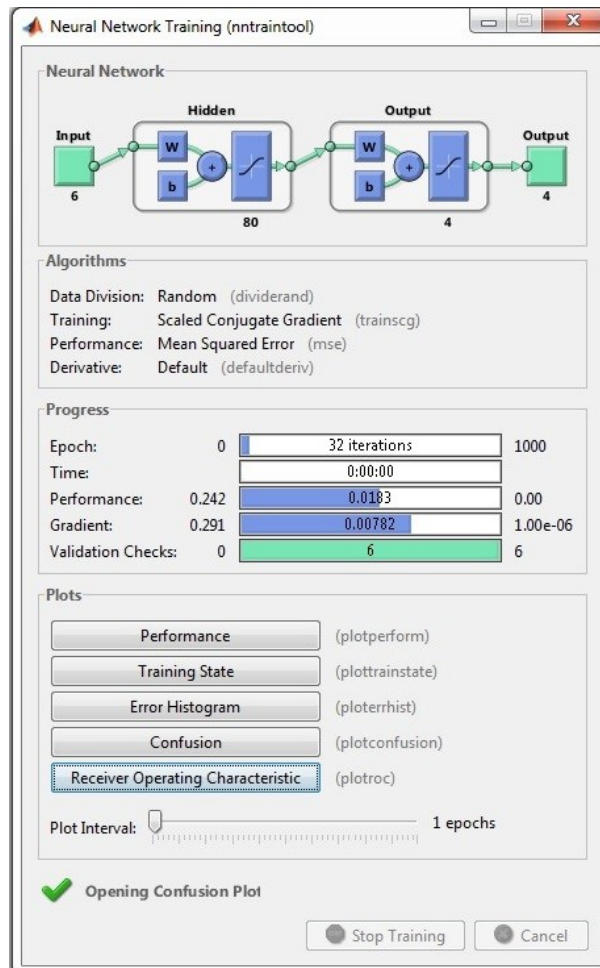


Fig. 10. The process of training a neural network



Fig. 11. Training results of the final ANN

3.3. Comparison of BNN with other algorithms

The BNN algorithm was compared with two other algorithms: K-Nearest Neighbors (KNN), a model that classifies data based on the k closest samples to the point being classified, and Logistic Regression, a statistical model used to classify data into two classes. The comparison used several criteria to assess classification accuracy: Area under the curve (AUC), classification accuracy (CA), the harmonic mean of precision and recall (F1 Score), precision, sensitivity or true positive rate (recall), and Matthew's correlation coefficient (MCC). The operations performed on the training samples can be summarized as follows:

- Embedding: Raw data is converted into digital representations (embeddings) that the model can better handle.
- Evaluation: Test and Score: Models are tested using data not used in training, and the results are recorded.
- Confusion Matrix: This table shows the model's performance by comparing the actual classifications with the expected classifications.
- Test Samples: New data used to evaluate the model's performance.
- Predictions: The results produced by the model are based on the data entered.

The results of the comparison were summarized in Tables 4-7.

Table 4. Stratified 5-fold Cross-validation

Model	AUC	CA	F1	Prec	Recall	Mcc
KNN	0.877	0.798	0.802	0.820	0.798	0.590
Logistic Regression	0.937	0.869	0.869	0.869	0.869	0.711
Neural Network	0.944	0.873	0.873	0.874	0.873	0.720

Table 5. Confusion matrix for logistic regression (showing the number of instances)

Actual	Predicted		Σ
	Normal	Osteoarthritis	
Normal	658	152	810
Osteoarthritis	155	1385	1540
Σ	813	1537	2350

Table 6. Confusion matrix for KNN (showing the number of instances)

Actual	Predicted		Σ
	Normal	Osteoarthritis	
Normal	658	152	810
Osteoarthritis	155	1385	1540
Σ	813	1537	2350

Table 7. Confusion matrix for neural network (showing the number of instances)

Actual	Predicted		Σ
	Normal	Osteoarthritis	
Normal	667	143	810
Osteoarthritis	155	1385	1540
Σ	822	1528	2350

According to these results, it is clear that the neural network technique is better and more accurate than the other two techniques.

4. Conclusion

The present study showed that using a back-propagation neural network (BNN) and pre-processing of digital images to predict osteoporosis using MATLAB based on several statistics gives a highly accurate result for identifying osteoporosis by distinguishing between healthy and diseased X-ray images. It can be applied to build an adjuvant system for orthopedic diseases. Training BNN on statistical outcomes is one of the most important factors by which normal bone disease and osteoporosis can be classified. It is possible to study other types of bone diseases, such as rickets, and apply the proposal in the study to them.

Acknowledgement

The authors would like to acknowledge the cooperation and assistance they received from the Baghdad Health Department, Al-Rusafa, and Al-Shaheed Al-Sadr General Hospital, to complete this research.

References

- [1] L. Pinto-Coelho, "How artificial intelligence is shaping medical imaging technology: A survey of innovations and applications". *Bioengineering*, vol. 10, no. 12, 2023. <https://doi.org/10.3390/bioengineering10121435>.
- [2] M.A. Simon, M.A. Aschliman, N. Thomas, H.J. "Limb-salvage treatment versus amputation for osteosarcoma of the distal end of the femur. *J Bone Joint*", *JBJS*, vol. 68, no.9, pp.1331–7, 1986. <https://doi.org/10.2106/00004623-198668090-00005>.
- [3] WHO, "Assessment of fracture risk and its application to screening for postmenopausal osteoporosis: report of a WHO study group [meeting held in Rome from 22 to 25 June 1992]", 1994. <https://apps.who.int/iris/handle/10665/39142>.
- [4] K. F. Janz, "2016 the year that was: bone strength," *Pediatric Exercise Science*, vol. 29, no. 1, pp. 23–25, 2017. <https://doi.org/10.1123/pes.2016-0279>.
- [5] D. J. Hunter and P. N. Sambrook, "Bone loss: epidemiology of bone loss," *Arthritis Research & Therapy*, vol. 2, no.6, pp.1-5, 2000. <https://doi.org/10.1186/ar125>.
- [6] J. S. Finkelstein, S. E. Brockwell, V. Mehta, "Bone mineral density changes during the menopause transition in a multiethnic cohort of women". *The Journal of Clinical Endocrinology & Metabolism*. vol. 93, no. 3, pp. 861–868, 2008. <https://doi.org/10.1210/jc.2007-1876>
- [7] L. Warming, C. Hassager, and C. Christiansen, "Changes in bone mineral density with age in men and women: a longitudinal study," *Osteoporosis International*. vol. 13, no.2, pp. 105–112, 2002. <https://doi.org/10.1007/s001980200001>.
- [8] S. L. Resmi, V. Hashim, J. Mohammed, and P. N. Dileep, "Bone Mineral Density Prediction from CT Image: A Novel Approach using ANN". *Applied Bionics and Biomechanics*, 2023. <https://doi.org/10.1155/2023/1123953>.
- [9] V. Kawade, V. Naikwade, V. Bora, and S. Chhabria, "A Comparative Analysis of Deep Learning Models and Conventional Approaches for Osteoporosis Detection in Hip X-Ray Images". In *Conf. Communication and Computing (WCONF)*, IEEE, pp.1-7, 2023. <https://doi.org/10.1109/WCONF58270.2023.10235129>.
- [10] T. Ramesh, and V. Santhi, "Multi-level classification technique for diagnosing osteoporosis and osteopenia using sequential deep learning algorithm". *International Journal of System Assurance Engineering and Management*, vol.15, no. 1, pp.412-428, 2024. <https://doi.org/10.1007/s13198-022-01760-9>.
- [11] S. Steffi, "Automated microaneurysms detection in retinal images using SSA optimised U-NET and Bayesian optimised CNN". *Computer Methods in Biomechanics and Biomedical Engineering: Imaging and Visualization*, vol. 11, no. 6, pp.2530-2546, 2023. <https://doi.org/10.1080/21681163.2023.2244603>.
- [12] G. Amiya, P. R. Murugan, K. Ramaraj, V. Govindaraj, M. Vasudevan, M. Thirumurugan, and A. Thiyagarajan, "LMGU-NET: methodological intervention for prediction of bone health for clinical recommendations". *The Journal of Supercomputing*, pp.1-28, 2024. <https://doi.org/10.1007/s11227-024-06048-2>.
- [13] S. Wang, X. Tong, Q. Cheng, Q. Xiao, J. Cui, J. Li, and X. Fang, "Fully automated deep learning system for osteoporosis screening using chest computed tomography images". *Quantitative Imaging in Medicine and Surgery*. vol.14, no. 4, 2024. <https://doi.org/10.21037/qims-23-1617>.
- [14] L. Gu, "Optimized backpropagation neural network for risk prediction in corporate financial management". *Scientific Reports*, vol. 13, no.1, 2023. <https://doi.org/10.1038/s41598-023-46528-8>.
- [15] G. K. Jha, "Artificial neural networks and its applications". IARI, New Delhi, girish_iasri@rediffmail. Com, 2007.
- [16] U. Farid dowl, J. DeGroot Anthony, R. parker sedny, and V. Rao Vermuri, "back-propagation neural networks: systolic implementation for seismic signal filtering". *neural networks*. vol. 1, no. 3, pp. 139-148, 1989.
- [17] R. O. Duda, P. E. Hart, and D. G. Stork. "Pattern Classification: Pattern Classification". John Wiley & Sons., Inc. 2000.
- [18] Mosalam, K. M., & Gao, Y., "Artificial Intelligence in Vision-Based Structural Health Monitoring". Springer, 2024.
- [19] K. D. Toennies. "Guide to medical image analysis". Springer-Verlag London Ltd. 2017.
- [20] B. Zafarifar, "Micro-codable discrete wavelet transform". *Computer Engineering Laboratory*, Delft University of Technology, 2002.
- [21] S. L. Resmi, V. Hashim, J. Mohammed, and P. N. Dileep, "Bone Mineral Density Prediction from CT Image: A Novel Approach using ANN". *Applied Bionics and Biomechanics*, no.1, 2023. <https://doi.org/10.1155/2023%2F1123953>.